

# Efficient Learning of Control Policies for Robust Quadruped Bounding using Pretrained Neural Networks

Anqiao Li<sup>\*1</sup>, Zhicheng Wang<sup>\*1</sup>, Jun Wu<sup>1</sup>, Qiuguo Zhu<sup>†1</sup>

**Abstract**— Bounding is one of the important gaits in quadrupedal locomotion for negotiating obstacles. However, due to a large number of robot and environmental constraints, conventional planning and control has limited ability to adapt bounding gaits on various terrains in real-time. We proposed an efficient approach to learn robust bounding gaits by first pretraining the deep neural network (DNN) using data from a robot that used conventional model-based controllers. Next, the pretrained DNN weights are optimized further via deep reinforcement learning (DRL). Also, we designed a reward function considering contact points to enforce the gait symmetry and periodicity, and used feature engineering to improve input features of the DRL model and the bounding performance. The DNN-based feedback controller was learned in simulation first and deployed directly on the real Jueying-Mini robot successfully, which was computationally more efficient and performed much better than the previous model-based control in terms of robustness and stability in both indoor and outdoor experiments.

## I. INTRODUCTION

Legged robots have been attracting more attention in recent years for their versatile motion capabilities. The motion planning and control of a legged robot has been well researched and the limitations are also well understood, i.e. model-based methods require prior knowledge and a non-trivial process of specifying and tuning parameters for the constraints, and the computational time is also not constant which is undesirable for hard real-time control. Hence, a learning-based approach, such as the deep reinforcement learning (DRL), has gained new trends in legged locomotion control to solve these problems, because it allows learning a MIMO (multiple input, multiple output) feedback control policies that can run in real-time, particularly dealing with very high dimensional sensory inputs.

Constrained by the capability of computing devices and legged robots, DRL has not been applied to motion control for quadruped robots until recent years. Haarnoja and Tan [1,2] first implemented DRL-trained walking, trotting, and galloping on a real Minitaur robot and verified the feasibility of the end-to-end route. Subsequently, Ha [3] utilized an on-robot DRL method with minimal human interference by constructing a physical reset mechanism quite similar to that of a computer simulation, and achieved trotting and walking on unstructured terrain. The work in [4-6] presents learning separate skills such as trotting and fall recovery using an end-

to-end DRL framework. To generate multiple locomotion skills within one framework, the multi-expert learning architecture (MELA) was proposed to fuse multiple neural networks into a synthesized one in real-time [7]. Tsounis [8] introduced DeepGait, a gait planner that can cross discrete terrain with a metachronal gait. With the help of a Timed Convolutional Network and contact state estimator, the robot conquered a series of challenging terrains using trotting [9]. To imitate real quadruped animals to the greatest extent, Peng [10-12] collected locomotion data from real dogs and achieved trotting and spinning in robots based on domain adaptation.

In addition to trot and gallop, bound gait is an important form of legged animal locomotion. It can be used to cross different obstacles and is often used as a transition model between trotting and galloping [13]. However, it is harder to achieve by DRL than trotting and galloping for several reasons. First, if the robot is primarily given a forward speed reward in DRL, it can easily be trained to perform a gallop gait. This is because gallop can help the quadruped robot gain the fastest speed. Conversely, to train a symmetrical dual-phase gait such as bounding and trotting, we need extra reward function terms to retain the consistency of corresponding legs. Second, even with a leg-consistency reward, it is still harder to train the bound gait than the trot. This is because the center of mass (CoM) and pitch angle of the robot change more violently when the robot is in bound gait. This usually causes falling, and terminates the training process. Hence, few teams have so far been able to generate bounding in a quadruped robot.

In this paper, we propose a solution to train a neural network controller through DRL that can perform a bound gait and be successfully transferred to the physical Jueying Mini robot. The main contributions of this paper can be summarized as follows:

1) To keep DRL optimization from falling into an unexpected locally optimal solution, we present a novel pre-fitting method. The initial weights of PPO2 are trained with robot state data collected from the robot using spring linear inverted pendulum (SLIP) model-based controller. With this method, the initial weights of Actor in PPO2 can converge more easily to the optimum, a bounding controller, as we expected.

2) Because of the violent fluctuations of the robot when bounding, we design a more effective reward function based on the control of contact points to replace the common reward function that encourages consistency in the legs. With this reward, we expect to avoid frequently terminated cases caused by backward falls of the robot during training.

3) To further improve the controller's performance, we use feature engineering to pre-process the input features. With this method, we can obtain a more stable controller for the physical robot on flat terrain.

<sup>\*</sup>These authors contributed equally to this work.

<sup>1</sup>Anqiao Li and Zhicheng Wang are with the Institute of Cyber-Systems and Control, Zhejiang University, 310027, China.

<sup>†</sup>Jun Wu and Qiuguo Zhu are with State Key Laboratory of Industrial Control Technology and the Institute of Cyber-Systems and Control, Zhejiang University, 310027, China. (Qiuguo Zhu is the corresponding author, email: qgzhu@zju.edu.cn)

The organization of this paper is as follows: In Section II, we introduce the overall structure of our pre-fitting method, the DRL algorithms, and pre-featuring details. In Section III, we validate the feasibility of a controller trained with our method on a physical robot and compare the results with those of conventional controllers. Finally, in Section IV, the conclusion, along with inspiration for future work, is stated.

## II. PLATFORM OVERVIEW



Figure 1. Jueying Mini quadruped robot

### A. Robot Platform

Our work is deployed on the Jueying Mini quadruped robot platform (see Fig. 1). The Jueying Mini is a 12-DOF quadruped robot (three DOFs per leg) that focuses on agility. With a weight of 22 kg and joints actuated by brushless electric motors, the Jueying Mini can perform various movements. Its technical specifications are listed in Table 1.

TABLE I. TECHNICAL SPECIFICATIONS OF THE JUEYING MINI

| Property Name            | Value           | Unit  |
|--------------------------|-----------------|-------|
| Body Size                | 0.7*0.4*0.5     | m     |
| Leg Length(thigh+shank)  | 0.22+0.25       |       |
| Hip Roll Joint Position  | -22.0~22.0      |       |
| Hip Pitch Joint Position | -158.0~28.0     | deg   |
| Knee Joint Position      | 38.0~163.0      |       |
| Hip Roll Joint Velocity  | -15.0~15.0      |       |
| Hip Pitch Joint Velocity | -18.0~18.0      | rad/s |
| Knee Joint Velocity      | -20.0~20.0      |       |
| Hip Roll Joint Torque    | 10.0(Peak 23.0) |       |
| Hip Pitch Joint Torque   | 10.0(Peak 26.0) | Nm    |
| Knee Joint Torque        | 17.0(Peak 41.5) |       |

### B. Modeling

Because the Jueying Mini robot has a all-elbow structure, we simplified the robot into a joint-link system comprising rigid links as legs and revolute joints. The coordinates of each link are located on its parent joint. The directions of all coordinates are the same when the robot is in the initial position. A simplified model of the robot and its coordinates are shown in Fig.2.

### C. Simulation Environment

We adopted RaiSim [14] as the dynamic simulation environment. Because of its unique method of calculating contact forces, RaiSim is much faster than other dynamic simulation software. A simplified robot model of the Jueying

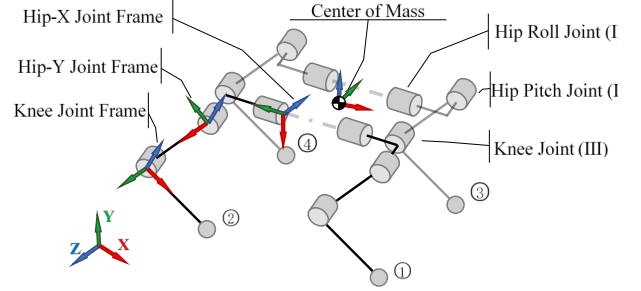


Figure 2. Simplified model of the Jueying Mini

Mini was implemented in the RaiSim environment with the corresponding controllers.

## III. METHOD

### A. Main Workflow of DRL

The main workflow of the training system is shown in Fig. 3. The observation data vector, also called the state vector, is retrieved from the simulation environment. It is a multi-dimensional vector comprising information about the robot itself.

The state vector is then sent to the deep neural network (DNN) as a frame of input, and the DNN instantly generates a corresponding frame consisting of a 12-dimensional output vector, which represents the expected joint positions.

A stable PD controller was used to convert the expected joint position into a 12-dimension expected joint torque vector. In addition to the basic PD torque, calculated with the joint position and velocity, an array of feedforward torques was added to the torque vectors to stabilize the robot system and help the joints move to the expected position more accurately. The feedforward torques are expected torques calculated with the expected states of the joints with floating-base inverse dynamics methods. The torque vector is sent to the robot in the simulation environment as commands. The work loop then repeats itself. When training the neural networks, input and output data vectors along with the reward values are stored in tuples for calculating the neural networks' weight offsets.

After the simulation training procedure, the neural network, which can perform well, is ready to be applied in an actual robot. The same structure, except for the training part, is deployed on the actual robot for offline running. Because of the difference between simulation and real robot systems, the real robot will be able to bound after the parameters have been slightly modified.

### B. Reinforcement Learning

The motion state of the robot  $s_t$  at a specific time is constrained by the previous state, therefore, the locomotion control is a Markov decision process, which is quite suitable for reinforcement learning (RL). The action  $a_t$  performed by the robot using policy  $\pi$  influences the probability distribution of the state transition, and the result of the transition leads to a corresponding reward value  $r_t$ , which

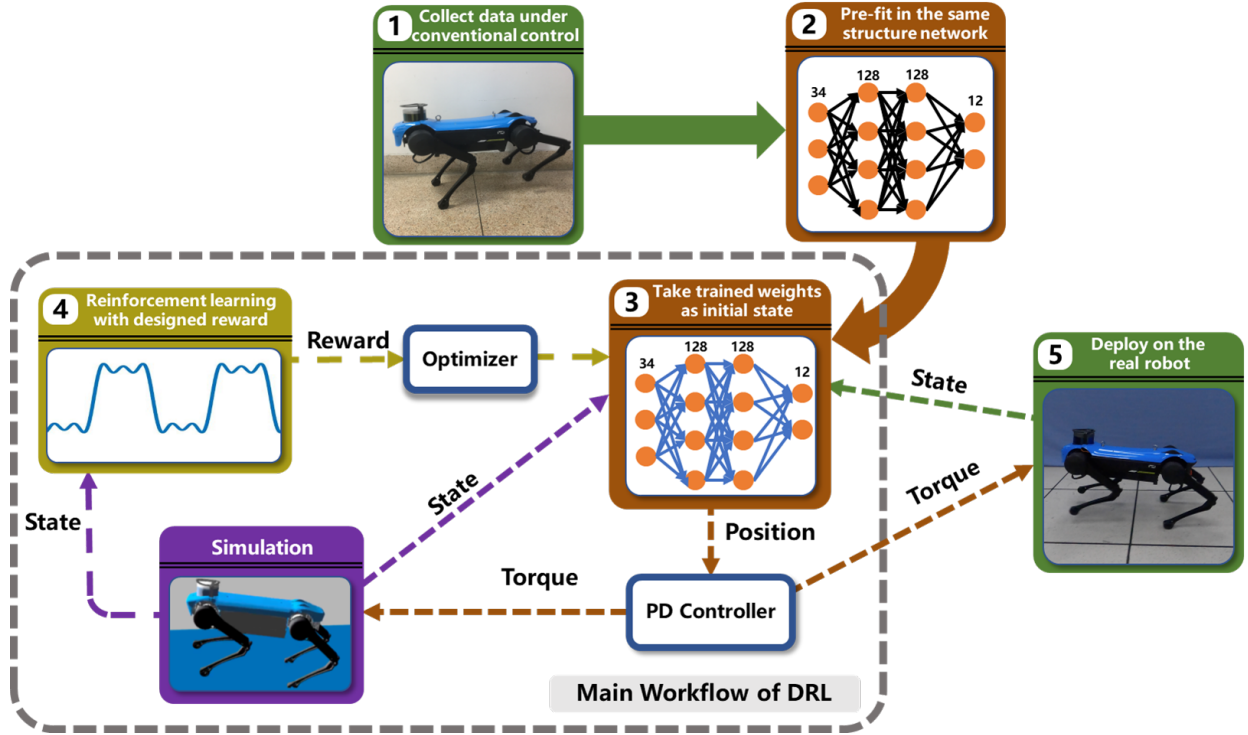


Figure 3. Overall training workflow. The overall workflow can be divided into two parts: the first part is pre-fitting (above grey box), and the second part is deep reinforcement learning (in the grey box). After training, the model is deployed on real robot (right side of grey box).

implies how successful the state is. Hence, optimizing the performance of the controller is equivalent to maximizing the discounted reward function.

$$\pi^*(\theta) = \underset{\theta}{\operatorname{argmax}} \mathbb{E}_{\tau(\pi(\theta))} \left[ \sum_{t=0}^{\infty} \gamma^t r_t \right] \quad (1)$$

In the formula above,  $\gamma$  is the discount factor, which implies that the importance of the reward value drops as time passes. In addition,  $\theta$  refers to the parameters in the policy; in our work,  $\theta$  represents the weights in the DNN. To train the DNN controller more quickly, we chose PPO2 [15-17] as the optimizer in our work.

### C. PF-DRL

There are two multi-layer perceptrons (MLP) deployed in the PPO2 algorithm, named the actor and critic. The structures of the neural networks are shown in Fig.3. With the random initialized weights, the model in the simulation did not perform the action we expected, but still obtained a high reward. The most common unexpected action is when the robot shakes its hind legs without any movement. We believe that the most possible reasons for this are that the optimization problem fell into a local optimum or our expected bound gait is not the global optimum. Instead of wasting effort adjusting each coefficient of the different rewards, we deployed the pre-fitting method, which is often used in deep learning to solve this problem, for example, a similar pre-training concept was used to pre-fit expert neural networks in the multi-expert learning framework [7].

Hence, we turned to conventional control for help. The observation space of RL is 34 dimensions, so we recorded

corresponding number of dimensions of data, e.g., the angle of each joint, when the robot bounded under conventional control.

After the data were collected, we constructed the neural network model with the same structure as the actor net of the RL model. We divided the recorded data as a training set and validation set. The input data of the neural network comprises 34 values recorded at the same time point and the label of each input includes the 12 target positions output by the conventional controller after 0.01 s, which is the control frequency in the RL simulation. We trained the neural network with different optimizers and learning rates in turn to minimize the mean squared error loss (Table 2).

TABLE II. TRAINING SEQUENCE

| optimizer | Learning rate | Training times |
|-----------|---------------|----------------|
| SGD       | 1e-2          | 500            |
| Adam      | 1e-3          | 500            |
| Adam      | 1e-4          | 500            |

When the loss is low enough for the following process, we then transferred the weights of the trained network into the actor net of the RL model as the initial state and started the training process directly. With this effort, after 4,000 training iterations, the model performed our expected bound gait.

### D. Reward Function

For RL processes, reward function is a vital factor in training. The RL algorithms will automatically find the trajectory that maximizes the total reward value. A proper reward function can improve the learning efficiency substantially. In our work the reward function comprises positive terms related to the main purpose of the movement such as the planar velocity of the whole robot, negative terms

(also called cost terms) to regulate the locomotion, and negative terms to restrict the energy cost and improve the safety of the robot (Table 3).

In Table 3,  $v_x^l$  refers to the speed of the robot base on axis  $x$  under frame  $l$ ,  $q_i$  and  $\tau_i$  refer to the position and torque of joint  $i$ , respectively,  $\phi$  refers to the pitch angle of robot torso,  $\tau(t)$  is the 12-dimensional torque vector at time  $t$ , and  $S(t)$  and  $G(i, t)$  are special functions that can be described as formula (2) and (3).

TABLE III. REWARD TERMS

| Reward              | Formula  | Coefficient Value   |
|---------------------|--|---------------------|
| Body Velocity       | $k( v_x^l ^2 +  v_y^l ^2)$                             | $k=160.0$           |
| Joint Torque        | $k \cdot \tanh(ct) \sum \tau_i$                        | $k=-0.002, c=0.04$  |
| Joint Velocity      | $k \cdot \tanh(ct) \sum \dot{q}_i$                     | $k=-0.0003, c=0.02$ |
| Gait                | $k \sum_{i=0}^3 S(t)G(i, t)$                           | $k=-50.0$           |
| Position Uniformity | $k( q_{LF} - q_{RF}  +  q_{LH} - q_{RH} )$             | $k=-0.01$           |
| Torque Uniformity   | $k( \tau_{LF} - \tau_{RF}  +  \tau_{LH} - \tau_{RH} )$ | $k=-0.001$          |
| Smoothness          | $k\ \tau(t) - \tau(t-dt)\ $                            | $k=-1e-6$           |
| Pitch Limitation    | $k( \phi )$ when $ \phi  > 0.3$                        | $k=20.0$            |

$$S(t) = \sin(\omega t) + \frac{1}{3} \sin(3\omega t) + \frac{1}{5} \sin(5\omega t) \quad (2)$$

$$G(i, t) = \begin{cases} 1 & \text{when foot } i \text{ touches ground} \\ 0 & \text{when foot } i \text{ does not touch ground} \end{cases} \quad (3)$$

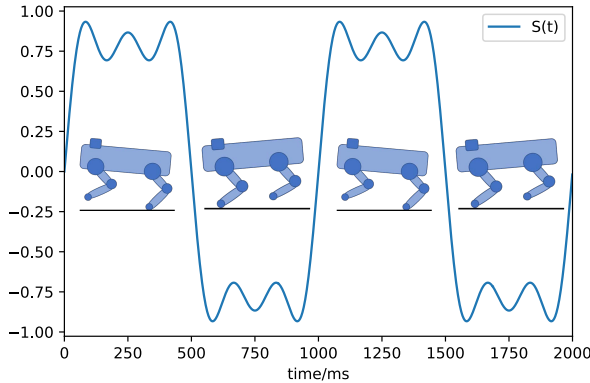


Figure 4. Gait signal plot. When robot acts as shown in the figure, it can get the maximum gait reward.

Meanwhile, to train the robot to perform the desired gait, we designed a special gait signal to instruct the robot to take steps at a specific frequency. The gait signal is periodic and zero-symmetric, and it uses a signed term to convert the foot contact state to a reward value. If the foot touches the ground at an undesired time, the negative gait signal will lead to a negative reward and increase the cost. In our work, we use a third-order superposition of trigonometric functions. This form of signal has a larger root mean square value (RMS) and is still differentiable, which can avoid the risk of non-convergence when using simple rectangle signals.

#### E. Feature Engineering

In the original version of our work, the observation vector comprises 34 basic variables related to the orientation of robot's torso and information about the joints (Table 4)

However, the trained controller did not perform well enough. The tested robot often fell on flat terrain. We assume the reason for this phenomenon is the MLP's lack of fitting ability. Hence, the technique of feature engineering, or so-called pre-featuring, was adopted to improve the gait.

TABLE IV. INDEX AND INPUTS OF THE NEURAL NETWORK

| Index Range | Input Name                                     | Unit               |
|-------------|--|--------------------|
| 0           | Robot Body Height                              | m                  |
| 1:4         | Z-Axis in World Frame Expressed in Robot Frame | rad                |
| 4:16        | Joint Position                                 |                    |
| 16:19       | Angular Velocity of Robot Body                 | rad/s              |
| 19:22       | Linear Acceleration of Robot Body              | m · s <sup>2</sup> |
| 22:34       | Joint Angular Velocity                         | rad/s              |

Inspired by feature engineering in data analysis, in which proper pre-featuring on the input data can improve the performance of the model by reducing the fitting stress for other modules and speed up the training process, we expanded the dimensions of the observation space to improve the performance. Because consistency of the front and hind legs is one of the most important features of the bound gait, we assume using the difference of each pair of legs can help regulate the locomotion. Therefore, we replace the Hip-Y and Knee joint positions with the difference in the two front legs' Knee and Hip-Y joint positions, and we make the same change for the two back legs. The deleted input features shown in formula (4), and the added pre-processed features can be described as formula (5).

$$q_{i,j}, (i = 1, 2, 3, 4; j = II, III) \quad (4)$$

$$q_{i,j} - q_{i+2,j}, (i = 1, 2; j = II, III) \quad (5)$$

#### F. Bridging the Sim-to-Real Gap

There are multiple gaps between the simulation environment and physical robots. These gaps are mainly due to measurement errors when the legged robot systems are modeled.

1. To overcome uncertainty in the robot model, we added stochastic noise to both the environment and robot parameters. The terrain in the simulation was also randomized. The noise coefficients are shown in Table 6.

TABLE VI. NOISE COEFFICIENTS

| Noise              | Standard Deviation | Unit |
|--------------------|--------------------|------|
| Link Mass          | $\pm 5$            | %    |
| Link Inertia       | $\pm 10$           | %    |
| Link CoM           | $\pm 7.5$          | cm   |
| Ground Friction    | $\pm 0.1$          |      |
| Ground Restitution | 0.15               |      |

2. We randomize the initial head direction every iteration. This is to prevent the neural network from overfitting to the head direction and terrain conditions.
3. To maintain the running frequency of the robot control system, we transform the weight data of neural network from a dedicated file format into universal csv format and run it forward with miniDNN, a C++ library, instead of using a Python framework.

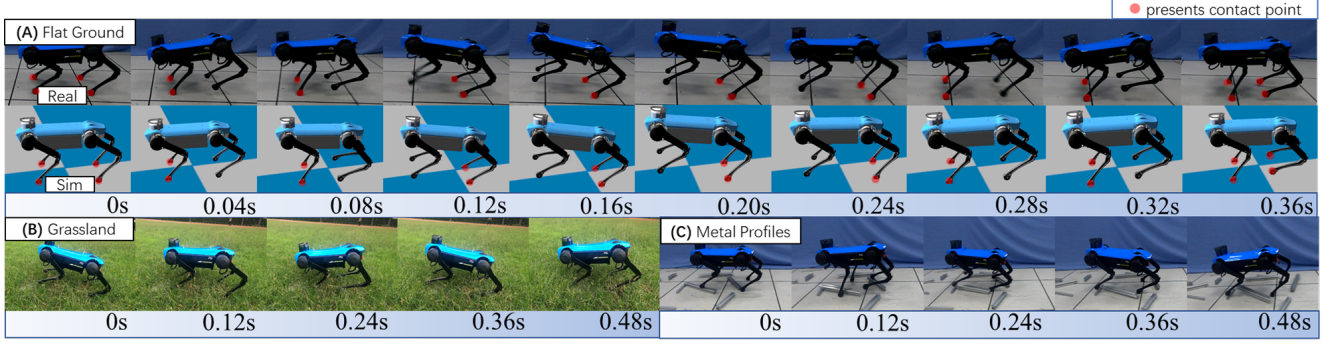


Figure 5. Snapshots of bounding in simulation and the real world. The trained model can be deployed successfully on real robot on flat ground(A). Furthermore, we test the robustness of the model on grassland and 3 cm metal profiles. In the unseen environment, the model also shows high stability.

#### IV. EXPERIMENTS

##### A. Simulation Result

The training platform on which we implemented our algorithm is a workstation with four Intel Xeon E2620 CPUs, 64 GB Memory, a Nvidia RTX 1080Ti GPU, and Ubuntu 16.04LS operating system. All results below were computed on this platform.

We applied deep pre-fitting methods on the actor network, and the training loss is shown in Fig. 6. After 1,500 iterations, the mean squared error loss on the training set was reduced to less than 0.007, and the network began to perform a premature bounding movement; however, an MLP with a simple structure was still unable to finish a cycle of bounding. Thus,

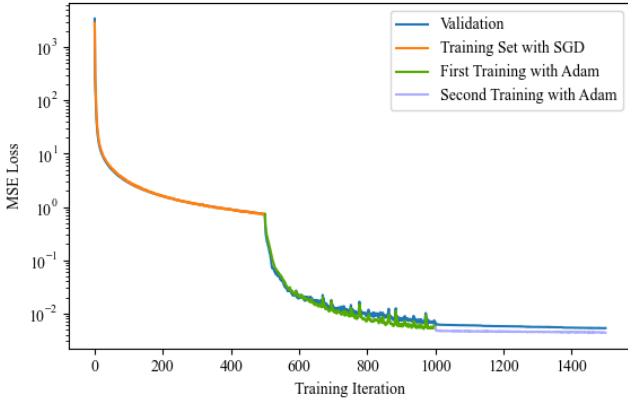


Figure 6. Training loss in the pre-fitting stage

the next step, the DRL, was needed.

The pre-fitted actor network, or so-called policy network, was then put into a simulation environment and optimized by DRL methods. We created 160 parallel RaiSim simulation environments that share the same policy network and trained them synchronously. Each environment had an iteration timestep of 2.5 millisecond, and torque commands were sent to the joints every two timesteps. This technique can substantially increase the efficiency of training for some multi-core computers. In our case, the simulation ran 700 times faster than real time when the simulation process was not visualized. Therefore, it took only 3 hours for the simulated robot to learn

to bound. The discounted reward function and loss is shown in Fig. 7.

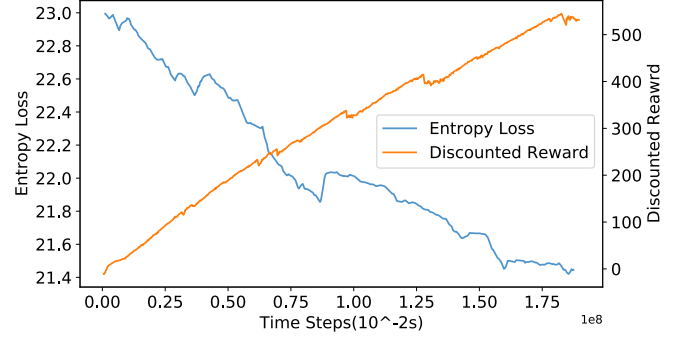


Figure 7. Episode reward value

After the two training steps above, the robot could perform the desired gait on a flat terrain in simulation. A plot of the joint position and joint torque is shown in Fig. 8. Here, we take the left hind leg of the Jueying Mini as an example. In the chart, it is apparent that every data plot has a frequency of 3 Hz, which means the robot takes three steps with the trained controller. The step frequency is consistent with the training dataset and gait reward.

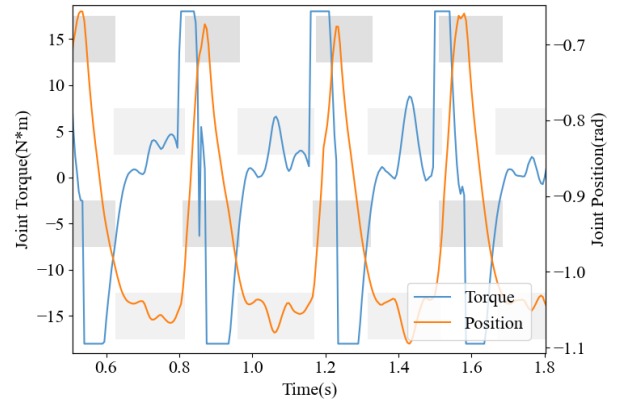


Figure 8. Joint position, torque and gait on real robot. Different rows of grey boxes means different contact states of each foot of robot. The first row and the third row represents forward two foot's contact states; the second row and the fourth row means the two backward foot's contact states.

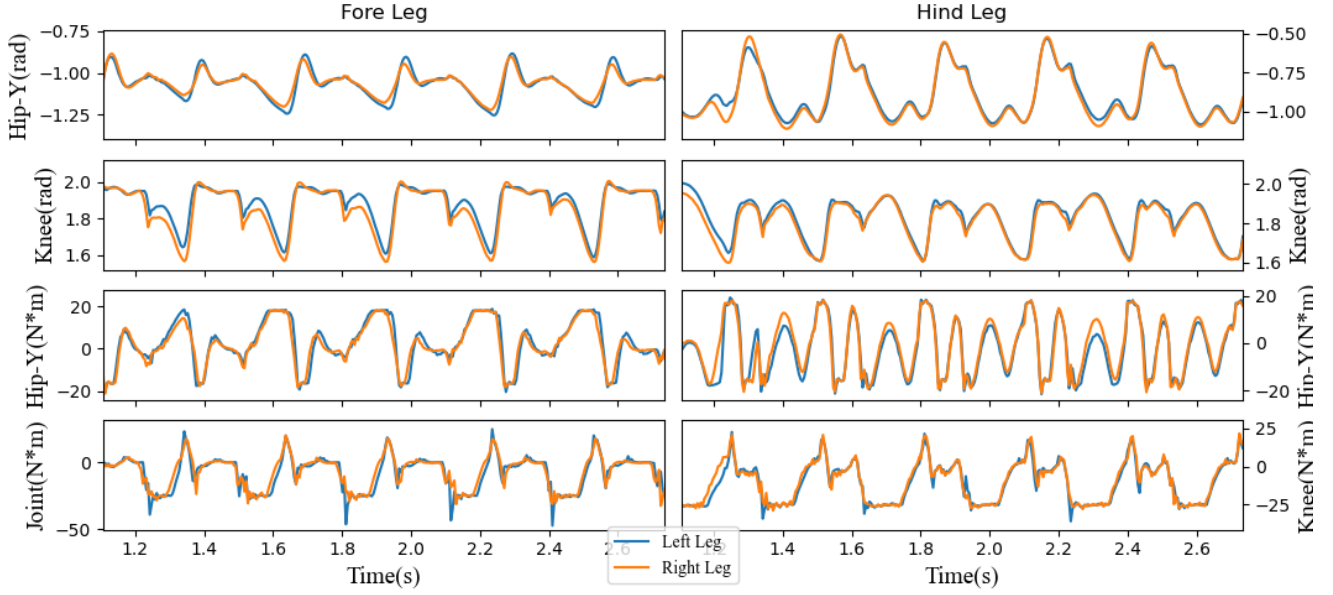


Figure 9. Runtime Plot of Joint Positions and Torques

### B. Real Robot Implementation

When the policy network was optimized enough to perform a continuous and agile bounding gait in simulation, it was ready to be transferred to real robots. The policy MLP was deployed on a physical Jueying Mini robot and reached a speed of 1.0 m/s on flat indoor terrain. The gait performed in the real world was identical to the simulated gait. The corresponding data plot is shown in Fig.9. Meanwhile, the controller showed sufficient robustness and ability to recover balance. The robot with the trained policy network was able to bound through unstructured terrain such as lush grassland and step over small obstacles about 4 cm in height. (Fig. 5(b))

With the same policy, the physical robot can also bound on complex discrete terrain. In the experiment, we put aluminum profiles of different shapes on the ground. With the same policy we trained using flat ground, the robot could bound through this complex terrain successfully (Fig.5(c)). In other words, when the contact point of the foot landed on an aluminum profile and negatively influenced the pose of the robot, the robot would adjust its pose to avoid slipping. This means that the policy we trained with RL is robust and has strong generalization ability.

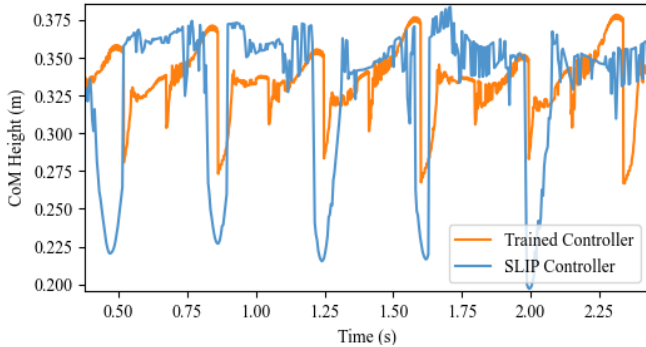


Figure 10. CoM height using different controllers

Compared with conventional controllers based on models, the trained neural network performs more smoothly when bounding. When the trained policy network controller is used, the height of the CoM changes in the range [0.25 m, 0.38 m] with a standard deviation of 0.020, whereas it fluctuates in the range [0.19 m, 0.41 m] with a standard deviation of 0.04 using when the conventional SLIP controller is used. The comparison plot is shown in Fig. 10.

### V. CONCLUSION

This paper presented a DRL-based control method to generate feedback control for the Jueying Mini robot which was able to achieve a bound gait in simulation and on the physical robot by a direct sim2real transfer. Using the same reward function, we can achieve a bound gait using a pre-fitting method or feature engineering. The former method provides a more robust model that can bound through complex terrain, while the latter one performed better on the flat ground.

With the pre-fitting method, we transferred the conventional controller to a neural network that could be modified by RL training. By changing coefficients of each reward, we were able to adjust the gait frequency more easily than with a conventional control method. Furthermore, we verified the feasibility of deploying a feature engineering method in DRL, which has previously commonly been used in deep learning.

Future work will consider ways of using PF-DRL to achieve more complex actions, like backflip, and changing the pre-fitted data source from conventional controller to human teaching. In addition, introducing more information into the input of the model is also worth exploring. In this study, we did not use the robot's camera and lidar systems, but they could provide more information about the state of the robot.

## REFERENCES

- [1] Haarnoja, Tuomas, et al. "Learning to walk via deep reinforcement learning." arXiv preprint arXiv:1812.11103 (2018).
- [2] Tan, Jie, et al. "Sim-to-real: Learning agile locomotion for quadruped robots." arXiv preprint arXiv:1804.10332 (2018).
- [3] Ha, Sehoon, et al. "Learning to Walk in the Real World with Minimal Human Effort." arXiv preprint arXiv:2002.08550 (2020).
- [4] Hutter, Marco, et al. "Anymal-a highly mobile and dynamic quadrupedal robot." 2016 IEEE/RSJ International Conference on Intelligent Robots and Systems (IROS). IEEE, 2016.
- [5] Hwangbo, Jemin, et al. "Learning agile and dynamic motor skills for legged robots." Science Robotics 4.26 (2019).
- [6] Lee, Joonho, Jemin Hwangbo, and Marco Hutter. "Robust recovery controller for a quadrupedal robot using deep reinforcement learning." arXiv preprint arXiv:1901.07517 (2019).
- [7] Yang, Chuanyu, et al. "Multi-expert learning of adaptive legged locomotion." Science Robotics 5.49 (2020).
- [8] Tsounis, Vassilios, et al. "Deepgait: Planning and control of quadrupedal gaits using deep reinforcement learning." IEEE Robotics and Automation Letters 5.2 (2020): 3699-3706.
- [9] Lee, Joonho et al. "Learning quadrupedal locomotion over challenging terrain." Science robotics 5 47 (2020)
- [10] Peng, Xue Bin, Glen Berseth, and Michiel Van de Panne. "Terrain-adaptive locomotion skills using deep reinforcement learning." ACM Transactions on Graphics (TOG) 35.4 (2016): 1-12.
- [11] Peng, Xue Bin, et al. "Learning Agile Robotic Locomotion Skills by Imitating Animals." arXiv preprint arXiv:2004.00784 (2020).
- [12] Peng, Xue Bin, and Michiel van de Panne. "Learning locomotion skills using deeprl: Does the choice of action space matter?." Proceedings of the ACM SIGGRAPH/Eurographics Symposium on Computer Animation. 2017.
- [13] G. C. Haynes and A. A. Rizzi, "Gaits and gait transitions for legged robots," Proceedings 2006 IEEE International Conference on Robotics and Automation, 2006. ICRA 2006., Orlando, FL, 2006, pp. 1117-1122, doi: 10.1109/ROBOT.2006.1641859.
- [14] Hwangbo, Jemin, Joonho Lee, and Marco Hutter. "Per-contact iteration method for solving contact dynamics." IEEE Robotics and Automation Letters 3.2 (2018): 895-902.
- [15] Konda, Vijay R., and John N. Tsitsiklis. "Actor-critic algorithms." Advances in neural information processing systems. 2000.
- [16] Schulman, John, et al. "Trust region policy optimization." International conference on machine learning. 2015.
- [17] Schulman, John, et al. "Proximal policy optimization algorithms." arXiv preprint arXiv:1707.06347 (2017).